

Document downloaded from:

<http://hdl.handle.net/10251/80104>

This paper must be cited as:

Verdú Amat, S.; Ivorra Martínez, E.; Sánchez Salmerón, AJ.; Grau Meló, R.; Barat Baviera, JM. (2016). Spectral study of heat treatment process of wheat flour by VIS/SW-NIR image system. *Journal of Cereal Science*. 71:99-107. doi:10.1016/j.jcs.2016.08.008.



The final publication is available at

<http://dx.doi.org/10.1016/j.jcs.2016.08.008>

Copyright Elsevier

Additional Information

Spectral study of heat treatment process of wheat flour by VIS/SW-NIR image system

Samuel Verdú^{1*}, Eugenio Ivorra², Antonio J. Sánchez², José M. Barat¹, Raúl Grau¹

¹Departamento de Tecnología de Alimentos. Universidad Politècnica de València, Spain.

² Departamento de Ingeniería de Sistemas y Automática, Universidad Politècnica de València, Spain

*Author for correspondence: Samuel Verdú

Address: Edificio 8G - Acceso F – Planta 0

Ciudad Politécnica de la Innovación

Universidad Politécnica de Valencia

Camino de Vera, s/n

46022 VALENCIA – SPAIN

E-mail: saveram@upvnet.upv.es

Phone: +34 646264839

Abstract

The capability of the VIS/SW-NIR (visible/ short wave near infrared) hyperspectral imaging system to characterize the heat treatment process of cake wheat flour was studied. Combinations of heat treatments of flour were run at different temperatures (80, 100 and 130°C) and for various times (10, 20 and 30 min). The resulting treated flours were analyzed by the imaging technique. The hyperspectral results, studied by multivariate statistical methods, showed a pattern evolution of the flours treated by different heat treatments. The wavelengths that contributed the most, and implied in the differentiations, were detected. The selection of wavelengths allowed us to optimize the analysis, which reduced from 54 to 6 wavelengths. To ensure that the VIS/SW-NIR information depended on the heat treatment influence on flours, cakes were produced and characterized according to height, mass loss during the baking process, crumb structure and textural properties. The VIS/SW-NIR imaging analysis was capable of following the changes that occurred during the different heat treatments of flours. VIS/SW-NIR was applied to determine and adjust the heat treatment process variables to improve the features of flours during the cake production process.

Keywords: heat treatment, wheat flour, VIS/SW-NIR, process control

1. Introduction

Cake is a good example of a food product obtained from a foam structure into which air has been introduced by a mixing process, which finally expanded and was fixed by the baking process (Wang et al., 2013). Consumer acceptance is based not only on a sweet taste as sponge texture is extremely important. Cake texture depends on a cake batter's gas-retention capability during and after mixing (Chesterton et al., 2013). Depending on this property, internal structure and maximum rising can considerably alter. Variations in gas-retention capacity terms are: size of the bubbles generated; total number of bubbles; distribution of bubbles across the liquid phase of the cake batter (Shibata et al., 2011). The above-cited differences relate to the properties of the raw material used in the formula, where polymeric molecules, such as proteins and starch, and their physicochemical state and amount, have a direct impact. One main influential factor is the formation of a functional network based on proteins provided by several components like egg, milk, flour, etc., and starch provided principally by flour. This network can have quite different properties depending on the types of these components. Apart from the role of proteins, the state of flour starch and its physicochemical features are other direct factors in network structures, as is their behavior during the process. Therefore, the amount of proteins and starch in selected formula, plus the changes produced by pre-treatments under physicochemical conditions, cause variations that could be interesting for improving or optimizing some processes and product variables.

In line with this, one of the most widely used procedures is to heat treat flours at different temperatures and from distinct moisture contents. Cake flours are often heat treated, and was widespread because the discontinuation of flour chlorination as a flour conditioning method (Sahin, 2008). This is a physical treatment method utilized to

modify the functional properties of native starch, and includes pasting characteristics, granule morphology, amylose leaching, textural properties, etc., which are particularly favorable for food applications (Lee et al., 2012; Sun et al., 2014). Studies into the effect of heat treatment on the physical and chemical features of wheat flours have been published by Guerrieri et al., (1996), Ozawa and Seguchi, (2006), but the precise mechanism by which heat treatment affects flour behavior has not yet been identified exactly by researchers of this area (Meza et al., 2011).

The main effects observed in cakes made with heat-treated wheat flour are increased gas retention and, hence, maximum caking rising, bubble size reduction and homogenization, due to an increase in batter viscosity, which can also induce an increase water-holding capacity while baking/treating cake batter. These effects contribute to improve high sugar ratio cakes formulas, where large proportions of sugar and liquid put stress on the structure-building components, tending to decrease in volume towards the end of baking and cooling time, resulting in cake collapsed, dense or dipped product (Chesterton et al., 2015). All this, in turn, contributes to prevent this collapse, giving improved product volume and stability, and the overall quality of the appearance and mouth sensation of end products (Neill et al., 2012).

For all these reasons, heat treatment of wheat flours is an important technique to improve wheat flour properties, and to match them to the requirements of each production process and end product standard. Thus, although there are patented methods such as the Russo and Doe (1970), using a temperature range of 100-115°C/ 60 min, works are still researching the influence of different heat treatments, temperatures and flour moisture combinations on the aforementioned effects to predict flour improvement models, and to avoid using other chemical additives to achieve this aim. Therefore, studying the changes undergone by wheat flour during heat treatment can be interesting

for optimizing this process if we take into account the required necessities of the production process.

When changes in wheat flour occur, near infrared reflectance imaging techniques offer interesting capabilities that can be applied to study them. Specifically, VIS/SW-NIR (visible and the short wavelength near infrared imaging analysis) has been used in many works focused to different aspects within cereal processing science area, such as to study the variability and properties of flours based on both protein and starch (Verdú et al., 2015a; Xing et al., 2011). In the case of grain and flour control, this technique has been used by Del Fiore et al., (2010) and Yao et al., (2008) to detect toxic fungus contaminations in maize and wheat, and by Verdú et al., (2016) to detect wheat flour adulterations with other cereals. On the other hand, non-image based infrared spectrometers has also been used to develop a large number of applications in this sense. For example, Shao et al., (2011) predicted protein and starch levels in wheat flour by studying the infrared information obtained with a spectrophotometer. In the same way, characterization of flours that consider their properties during the bread-making process (Li Vigni et al., 2009), prediction of pericarp thickness of sorghum whole grain (Guindo et al., 2016), classification of different types of flour batches (Cocchi et al., 2005), predictions of the milling and baking parameters of different wheat varieties (Jirsa et al., 2008), continuous characterizations of the bread dough leavening phase (Li Vigni and Cocchi, 2013), etc.

Therefore, this technique could represent a rapid non destructive method to study the changes that wheat flour undergoes during heat treatment. The main purpose of this work was to study the capability of the VIS/SW-NIR imaging system to characterize the effect of the heat treatment process on cake wheat flour prior to cake making, and to

secondarily select the most influential wavelengths to optimize hyperspectral information.

2. Material and Methods

2.1. Heat treatment of wheat flour

Wheat flour was obtained from a producer (Molí del Picó-Harinas Segura S.L, Valencia, Spain), which is sold as a “high-strength flour” for bakery products, sliced bread, plum cakes, etc. On a wet basis, it contained 15% of moisture, 10% of protein and 31% of wet gluten. Its alveographic parameters were W= 145 (strength (J^{-4})), P= 46 (maximum pressure (mm)), L=143 (extensibility (mm)), P/L = 0.31. The works of Neil et al., (2012) and Marston et al. (2016) were taken as a reference about time-temperature combinations and operation settings for heat treatments. Heat treatment was performed with forced convection hot air at three different temperatures (80, 100 and 130°C) and times (10, 20 and 30 min). Each treatment was carried out by spreading 300 g of untreated flour on a layer of a maximum thickness of 0.5 cm, distributed on a 60 x 30 x 2.5 cm aluminum pan, which was covered with baking paper. Process was carried out in a convection oven (Whirlpool, St. Joseph, MI). The time for stabilizing oven temperature was 1.5 minutes as a maximum for the lower heat treatment (80°C). Temperature was monitored with a digital thermometer (range 0-300°C, resolution 0.1°C, precision $\pm 0.2^\circ\text{C}$). During this process, moisture reduced from 15% to 10.5% (wet basis) as a maximum for 130°C/30 min. Loss of moisture was calculated according to the mass difference between weights from after and before the process. In order to recover the original moisture values, flours were placed into a chamber (KBF720 Binder Tuttlingen Germany) with controlled humidity and temperature (15% R.H. and

25°C). Flours remained inside the chamber for 48 h as this time was required to recover moisture if maximum loss occurred, which was 130°C/30 min. Finally, samples were softly milled in a food mixer blender (Thermomix® TM31, Vorwerk, Germany) to homogenize any oversized particles produced during the process. Moisture of flour samples was controlled after milling to ensure that it was not affected.

2.2. VIS/SW-NIR data acquisition and processing

Images of the wheat flour samples treated by different heat treatments were taken with a Photonfocus CMOS camera MV1-D1312 40gb 12 (Photonfocus AG, Lachen, Switzerland) and a SpecimImSpector V10 1/2" filter (Specim Spectral Imaging, LTD., Oulu, Finland), which works as a linear hyperspectral camera. The illuminant was an ASD illuminator reflectance lamp (ASD Inc, Boulder, USA), which produces stable illumination over the full working spectral range. Samples were prepared by placing 35 g of given flour into a glass Petri dish (10 cm diameter) to form an approximately 1-cm thick layer. Four dishes of each treated flours were prepared. Five images of each petri dish were acquired, at room temperature, by rotating 1.04 radians each time around its normal axis. Twenty image acquisitions of each treatment combination were finally obtained. The position of both, the camera and illuminant in relation to the sample, was always constant to control the lighting conditions and to obtain a constant image dimensions. In order to avoid any heat transfer to the sample, the distance between the illuminant and sample was 0.5 m. The distance between the camera and sample was 0.15 m. The obtained image (scanned line) was composed of 256 gray levels (8 bits). The diffuse reflectance spectrum was collected with 54 different wavelengths (each wavelength reflectance was digitalized with 8 bits). These wavelengths were distributed

at intervals of 11.2 nm within a range from 400 to 1000 nm. The scanned line comprised 1312 points, thus an image was recorded with a resolution of 1312 x 1082 pixels. The spatial resolution achieved with this setup was $7 \text{ m} \cdot 10^{-5}$. Image reflectance calibration and preprocessing were performed as described in (Verdú et al., 2015a), but it essentially acted as a reflectance calibration to normalize the nonlinear light source reflectance and Standard Normal Variety statistical preprocessing. The camera was operated by software that was developed based on SDK Photonfocus-GigE_Tools using the C++ programming language.

2.3. Cake processing

Sponge cakes were made by employing the heat-treated and non heat-treated wheat flours as a pattern. The components employed and percentages used were based on previous studies (Meza et al., 2011), with some modifications. The formula was based on 36% white sugar, 27% wheat flour, 14.5% water, 14% whole liquid egg, 4% skimmed milk powder, 2.8% refined sunflower oil, 1% baking powder and 0.6% salt. The skimmed milk powder composition was 32.5% proteins, 54.5% of carbohydrates, 1% lipids and 1.3% salt (Central Lechera Asturiana, SAT. Asturias, Spain). The whole liquid egg composition was 11% proteins, carbohydrates were negligible, 9.5% lipids, and the rest was water (Grupo Maryper de Alimentacion, SL, Spain). The refined sunflower oil had a maximum acidity of 0.2° (Koipesol Semillas S.L., Spain). The commercial baking powder was composed of sodium bicarbonate, disodium diphosphate, rice flour and monocalcium phosphate (Royal, Kraft Foods Inc. Germany), white sugar presented $\geq 99.8\%$ sucrose (Azucarera Ebro, S.L., Spain) and refined marine salt $\geq 97\%$ NaCl (Salinera Española, S.A., Spain). Cake preparation was based on Chesterton et al. (2015) and was as follows:

1. Dry ingredients (flour, sugar, skimmed milk powder, salt and baking powder) were placed into a food mixer (Thermomix® TM31, Vorwerk, Germany) and mixed to obtain a homogeneous powdery mix (1.5 minutes/ 50 rpm).
2. Liquid ingredients (water, oil and whole liquid egg) were added to the food mixer along with the dry ingredients and were all mixed for 1 minute at 105 rpm to generate a homogeneous mixture.
3. The produced mixture was whisked for 10 minutes at 550 rpm to incorporate air and to thus obtain cake batter.
4. 250 g of cake batter (approximately 1 cm high) were placed into a pre-greased metal mold (8x8x15cm) to be baked.
5. The metal molds were placed in the middle of the oven (530x450x340, grill power 1200W, internal volume 32L, Rotisserie, DeLonghi, Italy) plate, which was preheated to 180°C. The baking time was 35 minutes.

2.6. Characterization of cakes

In order to ensure that the heat treatments applied to the wheat flour influenced the physical properties of the end product, the following were studied: final height (A), mass loss during baking process (ΔMb), texture profile analysis (TPA) and average area of bubble in crumb (Bz). Mass loss during the baking process was calculated by the difference between the weight of the pre-baking batter and that of the finished cake (cooled at room temperature for 1 h), expressed as %. The TPA was performed following the method by (Miñarro et al., 2012). Six 12.5 mm-thick cross-sectional slices were obtained from the center of each cake. These slices were grouped to be analyzed in pairs to form 25-mm slices. Finally, three analyses of each cake were done with five

cakes from each heat treatment. A TPA was run in a TA-TX2 texture analyzer (Stable Micro Systems, Surrey, UK). A 25-kg load cell (cylindrical accessory of 35 mm diameter) was used. Assay speed was set at 1.7 mm/s to compress the cake crumb center to 50% of the initial height of the slices (25 mm). The time between compressions was 5 s. The studied parameters were: hardness (H), springiness (S), cohesiveness (C), gumminess (G) and chewiness (Ch). The cake height and crumb internal structure were studied by 2D image segmentation. Once baking had finished, four 1-cm-thick slices were obtained from the center of each cake. One side of each slice was captured with a scanner (Aficio™ MP C300-Ricoh. Tokyo. Japan) to be analyzed by the 2D image segmentation method described previously by (Verdú et al., 2015b). The height of each slice was measured in middle zone of cake width (4 cm from lateral extreme). Five cakes were baked from each treated flour, thus 20 crumb images were obtained. A large number of samples was necessary to ensure recognition patterns on the internal crumb structure images since wide variability is normally presented. Images were acquired at a resolution of 300 dpi. A black background was used in all the captures to improve contrast, and to enhance the cell wall structure and porosity measurements.

2.7. Statistical analysis

The heat treatment effect on wheat flour was evaluated by the VIS/SW-NIR spectra, which were formed by reflectance data of 54 wavelengths. Information about reflectances formed a multivariable data matrix, which was analyzed with a multivariate unsupervised statistical procedure, as is usual in NIR information studies, with the aim of obtaining the maximum information of dataset. The multivariate unsupervised statistical procedure was PCA (Principal Component Analysis). This method is used to

describe and reduce the dimensionality of a large set of quantitative variables to a low number of new variables, called principal components (PCs), which are the result of linear combinations of the original variables. The number of PCs was selected after considering the change in tendency on the scree plot, and also the accumulated percentage of explained variability above 75%.

The physical parameters of cakes (A , ΔMb , H , S , C , G , Ch and Bz) were studied by a one-way variance study (ANOVA). In those cases in which the effect was significant (P -value < 0.05), means were compared with Fisher's least significant difference (LSD) procedure.

Support Vector Machines (SVM) were used to study the relationship between the hyperspectral data of the treated flours and the physical parameters of cakes. They were used to carry out nonlinear regressions between both data sets. SVM are a powerful supervised learning methodology, based on the statistical learning theory, that are commonly used for spectral analyses (Boser et al., 1992).

The procedures were run with PLS Toolbox 6.3 (Eigenvector Research Inc., Wenatchee, Washington, USA), which is a toolbox extension in the Matlab 7.6 computational environment (The Mathworks, Natick, Massachusetts, USA).

1. Results

3.1. VIS/SW-NIR data acquisition and processing

Figure 1A shows the scores in the PCA space according to the time and temperature factors of the heat treatment (77.4% of captured variance). Data evolution occurred mainly across axis PC1 (Principal Component 1, 54% of captured variance), influenced

by the above factors. The control sample was situated on the positive extreme of PC1, whereas all the other samples were displaced gradually to the zero value and to the negative zone, where both heat treatment temperature and time increased. When a combinatorial effect of both factors was evaluated, the samples treated at 80°C for the three times were placed near the control sample in the positive PC1 zone, while the treatment at 130°C was located in the negative PC1 zone for all three treatment times. Therefore, the hyperspectral information was obtained by the image technique report differences in the PCA space, where differences in samples placement could be related to the various heat treatments applied.

In order to facilitate the observation made of the effect of temperature and time of treatments on the hyperspectral information, a plot that included the evolution of the PC1 scores according to these factors was constructed. Figure 2 shows the mean PC1 scores value for each heat treatment according to both factors. When the PC1 values for each temperature were adjusted to an equation, the slope showed an increase in the change rate among the treatment times depending on temperature (80°C = $5 \cdot 10^9$; 100°C = $8 \cdot 10^9$; 130°C = $1 \cdot 10^{10}$). Thus one example of the observed behavior was the mean score value for treatment 100°C/10 min, which fell between those obtained from 80°C for 20 and 30 min. Similarly, the score value for the 100°C/20 min treatment was situated between those at 130°C for 10 and 20 min, while the 100°C/30 min treatment appeared to overlap the 130°C/20 min one.

Table 1

Table 1. Results of physical properties of cakes.

<i>Heat-treatment</i>		<i>Texture and internal structure of cakes</i>								
<i>Temperature (C°)</i>	<i>time (min)</i>	<i>ΔMb</i>	<i>A</i>	<i>Bz</i>	<i>H(g)</i>	<i>S</i>	<i>C</i>	<i>G</i>	<i>Ch</i>	
<i>Control</i>	-	11.8 ± 0.3 c	8.7 ± 0.4 a	2.9 ± 0.3 d	61.6 ± 2.3 c	0.84 ± 0.01 a	0.67 ± 0.01 ab	41.7 ± 1.8 cd	35.4 ± 1.8 bc	
	10	10.5 ± 0.3 ab	8.7 ± 0.3 a	2.2 ± 0.3 bc	80.1 ± 8 d	0.86 ± 0.09 ab	0.66 ± 0.01 ab	53.1 ± 4.9 d	45.9 ± 7.2 cd	
	20	10.3 ± 0.3 ab	8.5 ± 0.1 a	2.0 ± 0.2 bc	75.8 ± 7.7 d	0.87 ± 0.05 ab	0.66 ± 0.01 ab	50.8 ± 4.9 d	44.2 ± 5.7 cd	
<i>80</i>	30	10.2 ± 0.3 a	8.4 ± 0.2 a	1.9 ± 0.1 b	71.6 ± 7.4 d	0.87 ± 0.01 b	0.67 ± 0.01 ab	48.4 ± 5 cd	42.5 ± 4.3 cd	
	10	10.3 ± 0.1 a	8.4 ± 0.1 a	1.5 ± 0.1 a	78.5 ± 6.5 d	0.88 ± 0.01 b	0.67 ± 0.01 ab	53.1 ± 4.4 d	47 ± 3.4 d	
	20	10.8 ± 0.2 b	8.7 ± 0.2 a	1.9 ± 0.1 b	71.1 ± 5.4 d	0.88 ± 0.01 b	0.67 ± 0.01 ab	47.9 ± 3.7 cd	42.3 ± 3.1 cd	
<i>100</i>	30	11.3 ± 0.3 bc	8.6 ± 0.2 a	2.3 ± 0.2 c	63.6 ± 4.3 cd	0.88 ± 0.01 b	0.68 ± 0.01 b	42.7 ± 3.0 c	37.6 ± 2.8 c	
	10	10.2 ± 0.3 a	8.7 ± 0.3 a	1.6 ± 0.1 a	67.9 ± 3.7 d	0.86 ± 0.01 ab	0.65 ± 0.01 a	44.7 ± 2.8 cd	38.9 ± 2.5 c	
	20	10.8 ± 0.3 ab	8.5 ± 0.2 a	2.0 ± 0.1 bc	52.9 ± 4.8 b	0.88 ± 0.01 b	0.68 ± 0.01 b	35.9 ± 3.4 b	31.5 ± 3.1 b	
<i>130</i>	30	11.4 ± 0.2 c	8.6 ± 0.2 a	2.4 ± 0.2 cd	38.0 ± 5.9 a	0.89 ± 0.01 b	0.71 ± 0 c	27 ± 4 a	24.2 ± 3.6 a	

Values and standard deviations of cakes properties; ΔMb = mass loss during the baking process (%); A= height (cm); Bz = average area of bubble in crumb ($m^2 \cdot 10^{-6}$), H = hardness (g); S = springiness; C = cohesiveness; G = gumminess; Ch = chewiness. Values followed by different letters were significantly different at $P < 0.05$ in columns.

With the aim of evaluating which spectra zones were related with these changes in flour due to heat treatment, the PCA loadings were analyzed. Loadings were calculated according to the correlation between the original variables (wavelengths) and the principal components. Therefore, the original variables with a higher value of loadings in either the positive or negative correlation to a given component meant a heavy weight in the explanation of the variability explained by that principal component. As there were two variables, temperature and time, and after considering the differences between slopes in the above studied PCA, a decision was made to obtain three new PCAs based on the same data set, but a different one for each individual temperature. Here the objective was to view the evolution of the importance of the original variables influenced by an increase in temperature. Therefore, three new different PCAs were generated: PCA1 (80°C: 10, 20 and 30 min), PCA2 (100°C: 10, 20 and 30 min) and PCA3 (130°C: 10, 20 and 30 min). These PCAs were compared in loading weight terms. Figure 3 shows the loadings for component PC1, which gave the widest variance

in the three new PCAs, and generated a spontaneous data clustering according to treatment time.

It is important to note that all the loadings presented the same tendency for the spectra zones. The loadings of the visible spectra zones (400-700 nm) were situated mainly toward the positive values, whereas the SW-NIR zone (700-1000 nm) was situated toward the negative ones. This distribution meant that the wavelengths from both spectra zones provided inverted contributions to the variability explanation collected in PC1. The differences observed between the spectra zones obtained from the different heat treatments affected the loadings of each wavelength by increasing or decreasing the weight of the specific zone spectra in the explanation of the variability collected in PC1.

Hence the influence of heat treatments on flour reflectance was observed by evaluating the progress of the loadings from PC1, presented by each temperature (Figure 3A, 3B and 3C). First, high loadings for the wavelengths were observed from the visible zone, which meant that this spectra zone helped account for most of the variability obtained in PC1; specifically the wavelengths around 600 nm presented the common maximum value for them all, regardless of temperature. Variations on values among the temperatures were observed within the 411-490 nm and close to 700 nm zones. These variations could be attributed to color changes, principally around 700 nm (deep red and brown tones) due to chemical reactions between compositional proteins and starch, producing a spectrally detectable browning.

In the SW-NIR zone, the common maximum contribution was observed at around 780 nm for them all, regardless of temperature. There were also zones where differences among the temperatures were observed. These spectrum zones presented different areas where changes were differentiated (700-770 and 800-900) and related with the various

functional groups (Murray, 2004). The interval between 700 and 770 nm presented variations among temperatures and corresponded to the 3rd overtone of O-H, and also to a recognized water influential zone (Sinelli et al., 2006). It also represented the 4th overtone of C-H, in addition to a CH₂ influential zone (Li Vigni and Cocchi, 2013). These zones are related with modifications in the state of water in relationship to the other components and their physical changes such as starch (Chen et al., 2006). In this work, no changes in the concentrations of the flour components were made because only a physical treatment was applied to flours. So any changes in the reflectance in these wavelengths could be attributed to differences in the water and the rest of components states between the treated samples and the control sample. Thus, a possible explanation is that the changes in conformation of starch granule underwent by heat treatment could modify the interaction of radiation with both O-H and C-H groups of starch polymers, both amylose and amylopectin (Jirsa et al., 2008). The 800-900 nm interval also presented differences among temperatures, and in relation to the 3rd overtone of N-H; in other words, primary and secondary amines (Kimiya et al., 2013). The variations in loadings within this range were similar to the above range. Their weight increased toward negative values with a rise in temperature. The most marked change noted among temperatures was detected for 859 and 892 nm. The interpretation of this change in loadings could refer to the modifications undergone by proteins during heat treatment. The interaction between the amine groups from proteins and radiation could be modified when heat treatment was stronger because the original tridimensional structure of flour proteins (secondary, tertiary or quaternary) could have altered.

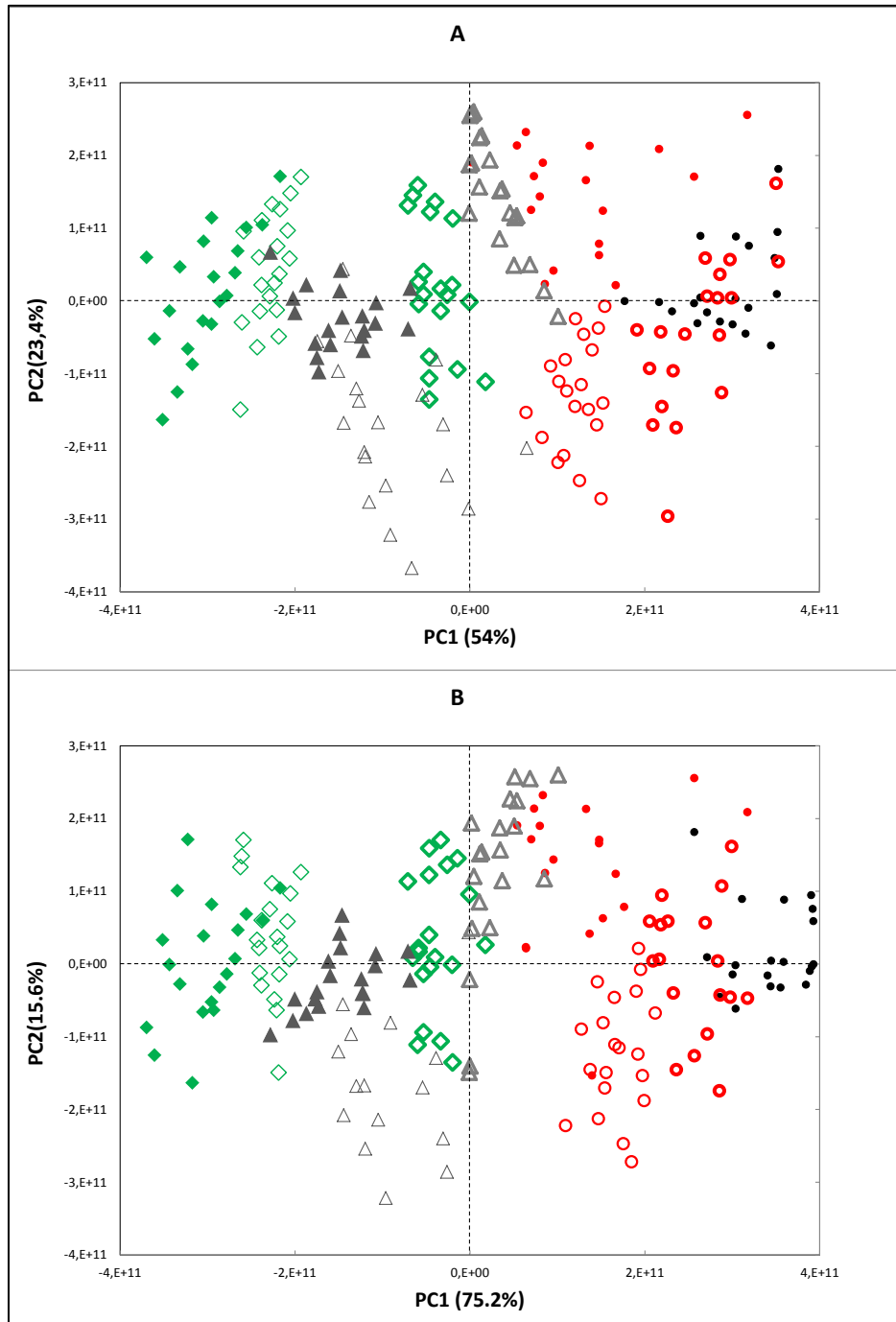


Figure 1. A: The PCA space obtained based on the reflectance of the SW-NIR imaging from wheat flour samples with different heat treatments. B: The PCA space obtained based on the reflectance of the six selected wavelengths. Colors of series correspond to different heat treatments temperatures: black, control flour (●); red 80°C (○ 80°C/10 min; ○ 80°C/20 min; ● 80°C/30 min); gray 100°C (▲ 100°C/10 min; △ 100°C/20 min; ▲ 100°C/30 min); green, 130°C (□ 130°C/10 min; □ 130°C/20 min; ■ 130°C/30 min).

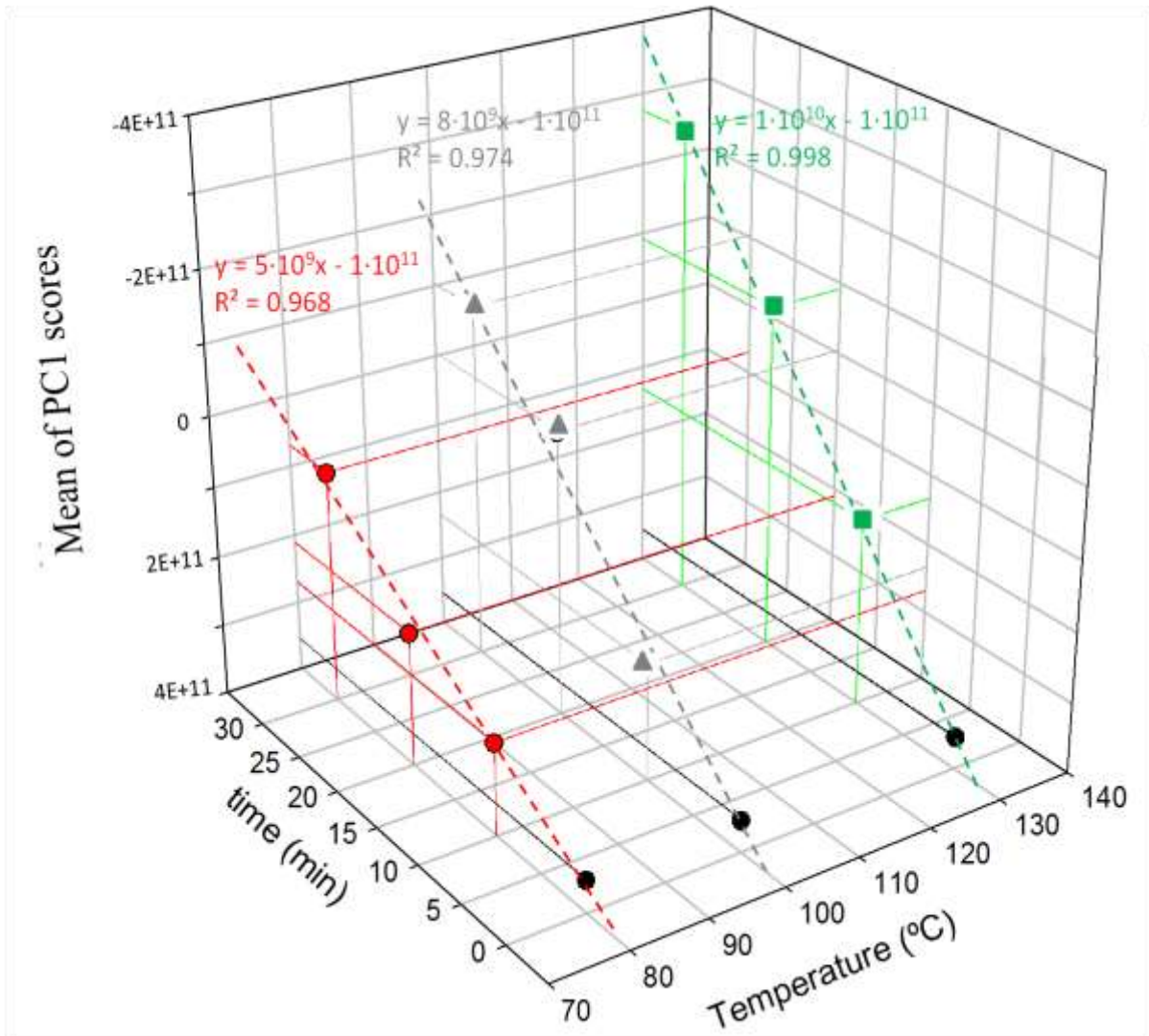


Figure 2. Representation of the mean of the scores for each temperature and heat treatment time, and the correlation index and the equation of the described line. Colors of the series correspond to different heat treatment temperatures: black, control flour (●); red 80°C (○ 80°C/10 min; ◐ 80°C/20 min; ◑ 80°C/30 min); gray 100°C (▲ 100°C/10 min; ◐ 100°C/20 min; ◑ 100°C/30 min); green 130°C (◐ 130°C/10 min; ◑ 130°C/20 min; ◒ 130°C/30 min). Points of the control flour were positioned only in relation to the mean score axis.

3.3 Reducing number of wavelengths

Having established that the hyperspectral information was able to characterize differences in heat treatments, dimensionality was reduced through wavelength

selection. The aim of wavelength selection was to select the optimal wavelengths that contained important information on quality attributes, and to make as few errors as possible for qualitative discriminations or quantitative determinations (Wu and Sun, 2013). The elimination of irrelevant variables can predigest calibration modeling and improve results in accuracy and robustness terms (Wu et al., 2008). Thus as reducing the number of wavelengths to obtain the same result for spontaneous heat treatments differentiation (Figure 1A) was the objective, we found that some wavelengths included mainly irrelevant information and did not improve model performance.

The wavelength selection criterion was based on the previous observations of loadings in Figure 3. As the characterization of heat treatments was influenced by the contribution level for specific wavelengths, those wavelengths with a higher contribution increment according to temperature were searched. To this end, loadings increment ($\Delta Loadings$) was calculated between the lower temperature (80°C) loading values and the other treatments, thus two loadings incremented the values for each wavelength (Figure 4). Maximum increments were observed within the previously defined wavelength ranges. Although almost all the wavelengths increased, the most important ones fell within the ranges previously established in Figure 3. The most marked peaks within these ranges were assumed to be the variables with the highest contribution to characterize heat treatments. The number of wavelengths was minimum to equate the result generated with the complete spectra (Figure 1A). Six wavelengths were finally selected, as indicated in Figure 4 (433, 456, 713, 736, 859 and 892 nm).

As observed in Figure 1B, the same spontaneous clustering distribution of samples across PC1 was observed by employing only these six selected wavelengths. The relative position of the treated flours across PC1 was the same in both cases. Even the results maintained the effect observed in Figure 2 for the increase in slope for the

change rate among the treatment times according to temperature. It was possible to condense the information from 54 to 6 wavelengths through wavelength selection by studying the loadings method.

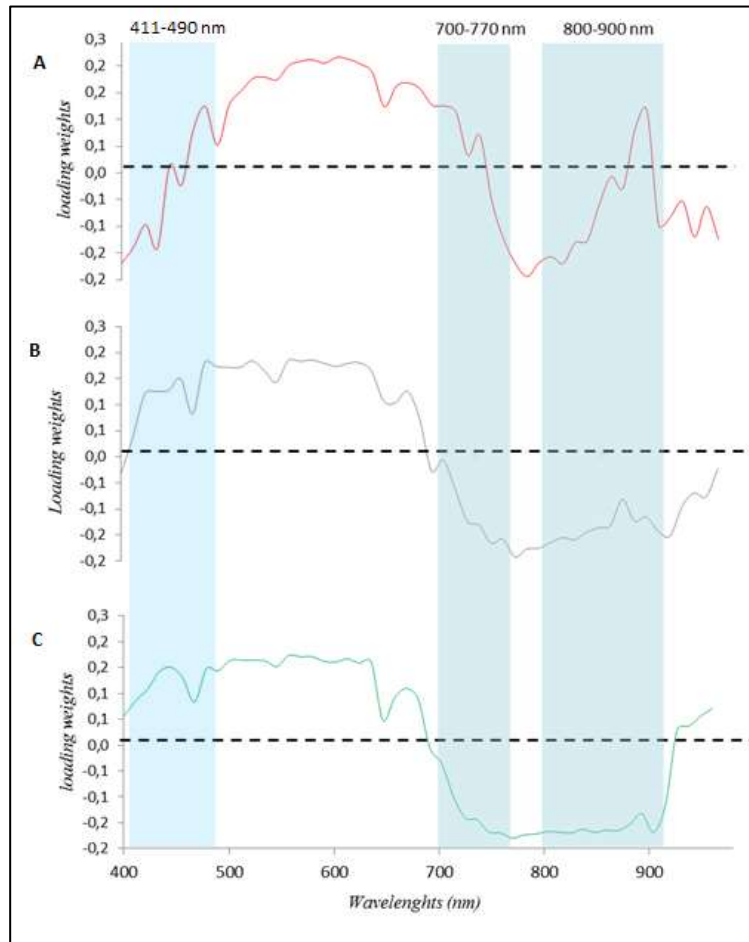


Figure 3. Loadings of PC1 for each heat treatment temperature. A: PCA1 isolated loadings of the 80°C heat treatments; B: PCA2 isolated loadings of the 100°C heat treatments, C: PCA3 isolated loadings of the 130°C heat treatments. Water marks indicate the regions with marked changes between treatments.

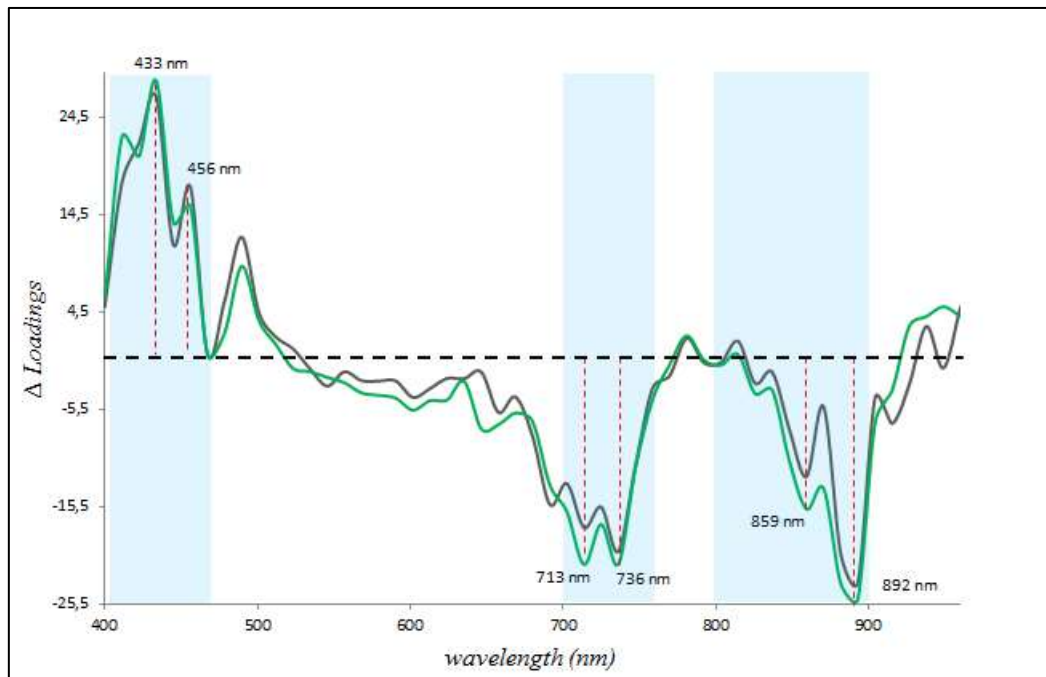


Figure 4. Loadings increment for each wavelength from each temperature PCA. Red dashed lines represent the selected wavelengths. Colored series represent the increments of the PC1 loadings of heat treatments at 100 (PCA2) and 130°C (PCA3) compared to 80°C (PCA1). Gray: loadings increment for the 100°C heat treatment, Green: loadings increment for the 130°C heat treatment. Water marks indicate the regions with maximum increments across the spectrum.

3.4 Relationship between information from the VIS/SW-NIR analysis and sponge cake properties

After ensuring that the hyperspectral information was capable of recognizing the factors related to changes that took place in flours during heat treatments, cakes were produced using those treated flours to ensure that the influence of the heat-treated flour on cakes reported by other authors (Chesterton et al., 2015; Meza et al., 2011) was repeated in this case.

The results of the physical cake properties are included in Table 1, where the influence of the heat treatment of flour on several cake properties is seen. Mass loss during the baking process (ΔMb) showed a drop, together with an increase of both temperature and time during the heat treatment, but not in all cases. The cakes made with the flours treated at 80°C presented statistical differences compared with the controls in all three cases, and their ΔMb lowered. The effect was inverse when treated for 30 min at 100 and 130. No differences were observed for height (A). For B_z , the tendency of the results was similar to ΔMb . The flour treated at 80°C obtained lower B_z values compared to the control. For the flours treated at 100°C and 130°C, which came close to the values of the control, those treated for 20 min and 10 min obtained the lowest B_z values. Differences in texture properties were also observed. The hardness, gumminess and chewiness of cakes increased when compared to the control, which they also did with the flour treated for 10 min, and regardless of the temperature used. However these parameters reduced at 20 and 30 minutes, and lower values were obtained for 130°C/20 min and 30 min. Cohesiveness lowered for 80°C and 100°C at all the tested times, but an increment at 130°C/30 min was observed. Overview, the results of the physical cake properties proved that the tested heat treatments modified samples, exactly as previous authors have described.

Finally, in order to prove the dependency noted between the reduced hyperspectral information and the set of cake properties, non linear regression was carried out based on the SVM technique. For this purpose, the complete data of the physical cake properties was used as independent multivariable matrix (X axis input), and the scores obtained from the PCA performed using the selected wavelengths (Figure 1B), were used as dependent variable (Y axis input). Non linear regression was done based on nu-SVM and the radial basis function as the kernel type, where 58 support vectors were

used. The R^2 of calibration was 0.992, while that of cross-validation was 0.985. This result reported a model that evidences the relationship and dependency between the hyperspectral information and cake features. Figure 5 shows the correlation between the observed PCA scores obtained with the hyperspectral information and those predicted from the physical cake properties. Despite the number of samples being insufficient for developing a model to predict the behavior of cakes, it sufficed to conclude that the used VIS/SW-NIR image system was able to obtain information from which it was possible to characterize heat treatment on cake wheat flours, which could be used to develop robust prediction models to process the control and optimization of end products.

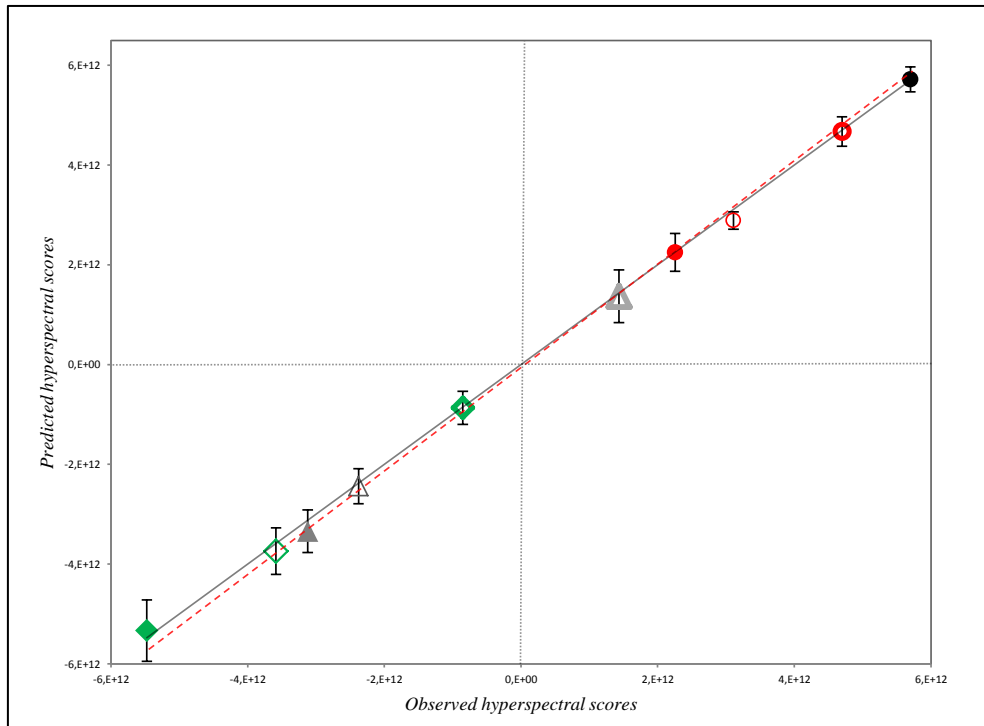


Figure 5. Correlation between Observed scores from the hyperspectral information PCA and those predicted from physical cake properties matrix by Support Vector Machines (SVM) method. Colors of the series correspond to different heat treatment temperatures: black, control flour (●); red 80°C (○ 80°C/10 min; ○ 80°C/20 min; ● 80°C/30 min); gray 100°C (▲ 100°C/10 min; △ 100°C/20 min; ▲ 100°C/30 min); green, 130°C (□ 130°C/10 min; □ 130°C/20 min; ■ 130°C/30 min). The black line means fit 1:1 and the red line means data fit. Vertical bars mean standard deviation.

5. Conclusions

The VIS/SW-NIR imaging system was capable of obtaining information about the diffuse reflectance spectrum from the treated flour and of characterizing different heat treatments according to time and temperature. The effect of the different heat treatments applied to flour led to a difference in the specific wavelength reflectance, which may relate to the main modifications undergone by flour components. The wavelengths that contributed the most, and were implied in the differentiations, were detected. The

selection of wavelengths allowed us to optimize the analysis, which reduced from 54 to 6 wavelengths. Dependency between the hyperspectral information of flour and cake properties with these flours was observed. These results indicated that the VIS/SW-NIR imaging system was capable of obtaining spectral information about the changes that took place during heat treatments with flour, which can be the base to determine and adjust process variables in order to improve the behavior of flours in different cake production phases. This method could be the basis to develop a analysis tool to help control and optimize online flour heat treatments.

6. References

- Boser, B.E., Guyon, I.M., Vapnik, V.N., 1992. A Training Algorithm for Optimal Margin Classifiers, in: Proceedings of the 5th Annual ACM Workshop on Computational Learning Theory. pp. 144–152. doi:10.1.1.21.3818
- Chen, Z.-P., Morris, J., Martin, E., 2006. Extracting chemical information from spectral data with multiplicative light scattering effects by optical path-length estimation and correction. *Anal. Chem.* 78, 7674–81. doi:10.1021/ac0610255
- Chesterton, a. K.S., de Abreu, D. a. P., Moggridge, G.D., Sadd, P. a., Wilson, D.I., 2013. Evolution of cake batter bubble structure and rheology during planetary mixing. *Food Bioprod. Process.* 91, 192–206. doi:10.1016/j.fbp.2012.09.005
- Chesterton, a. K.S., Wilson, D.I., Sadd, P. a., Moggridge, G.D., 2015. A novel laboratory scale method for studying heat treatment of cake flour. *J. Food Eng.* 144, 36–44. doi:10.1016/j.jfoodeng.2014.07.011
- Cocchi, M., Corbellini, M., Foca, G., Lucisano, M., Pagani, M.A., Tassi, L., Ulrici, A., 2005. Classification of bread wheat flours in different quality categories by a wavelet-based feature selection/classification algorithm on NIR spectra. *Anal. Chim. Acta* 544, 100–107. doi:10.1016/j.aca.2005.02.075
- Del Fiore, A., Reverberi, M., Ricelli, A., Pinzari, F., Serranti, S., Fabbri, A.A., Bonifazi, G., Fanelli, C., 2010. Early detection of toxigenic fungi on maize by hyperspectral imaging analysis. *Int. J. Food Microbiol.* 144, 64–71. doi:10.1016/j.ijfoodmicro.2010.08.001

- Guerrieri, N., Alberti, E., Lavelli, V., Cerletti, P., 1996. Use of spectroscopic and fluorescence techniques to assess heat-induced molecular modifications of gluten. *Cereal Chem.* 73, 368–374.
- Guindo, D., Davrieux, F., Teme, N., Vaksman, M., Doumbia, M., Fliedel, G., Bastianelli, D., Verdeil, J.L., Mestres, C., Kouressy, M., Courtois, B., Rami, J.F., 2016. Pericarp thickness of sorghum whole grain is accurately predicted by NIRS and can affect the prediction of other grain quality parameters. *J. Cereal Sci.* 69, 218–227. doi:10.1016/j.jcs.2016.03.008
- Jirsa, O., Hrušková, M., Švec, I., 2008. Near-infrared prediction of milling and baking parameters of wheat varieties. *J. Food Eng.* 87, 21–25. doi:10.1016/j.jfoodeng.2007.09.008
- Kimiya, T., Sivertsen, A.H., Heia, K., 2013. VIS/NIR spectroscopy for non-destructive freshness assessment of Atlantic salmon (*Salmo salar* L.) fillets. *J. Food Eng.* 116, 758–764. doi:10.1016/j.jfoodeng.2013.01.008
- Lee, C.J., Kim, Y., Choi, S.J., Moon, T.W., 2012. Slowly digestible starch from heat-moisture treated waxy potato starch: Preparation, structural characteristics, and glucose response in mice. *Food Chem.* 133, 1222–1229. doi:10.1016/j.foodchem.2011.09.098
- Li Vigni, M., Cocchi, M., 2013. Near infrared spectroscopy and multivariate analysis to evaluate wheat flour doughs leavening and bread properties. *Anal. Chim. Acta* 764, 17–23. doi:10.1016/j.aca.2012.12.018
- Li Vigni, M., Durante, C., Foca, G., Marchetti, a, Ulrici, a, Cocchi, M., 2009. Near infrared spectroscopy and multivariate analysis methods for monitoring flour performance in an industrial bread-making process. *Anal. Chim. Acta* 642, 69–76. doi:10.1016/j.aca.2009.01.046
- Marston, K., Khouryieh, H., Aramouni, F., 2016. Effect of heat treatment of sorghum flour on the functional properties of gluten-free bread and cake. *LWT - Food Sci. Technol.* 65, 637–644. doi:10.1016/j.lwt.2015.08.063
- Meza, B.E., Chesterton, A.K.S., Verdini, R. a., Rubiolo, A.C., Sadd, P. a., Moggridge, G.D., Wilson, D.I., 2011. Rheological characterisation of cake batters generated by planetary mixing: Comparison between untreated and heat-treated wheat flours. *J. Food Eng.* 104, 592–602. doi:10.1016/j.jfoodeng.2011.01.022
- Miñarro, B., Albanell, E., Aguilar, N., Guamis, B., Capellas, M., 2012. Effect of legume flours on baking characteristics of gluten-free bread. *J. Cereal Sci.* 56, 476–481. doi:10.1016/j.jcs.2012.04.012
- Neill, G., Al-Muhtaseb, A.H., Magee, T.R. a., 2012. Optimisation of time/temperature treatment, for heat treated soft wheat flour. *J. Food Eng.* 113, 422–426. doi:10.1016/j.jfoodeng.2012.06.019

- Shao, Y., Cen, Y., He, Y., Liu, F., 2011. Infrared spectroscopy and chemometrics for the starch and protein prediction in irradiated rice. *Food Chem.* 126, 1856–61. doi:10.1016/j.foodchem.2010.11.166
- Shibata, M., Sugiyama, J., Tsai, C.L., Tsuta, M., Fujita, K., Kokawa, M., Araki, T., 2011. Evaluation of viscoelastic properties and air-bubble structure of bread containing gelatinized rice. *Procedia Food Sci.* 1, 563–567. doi:10.1016/j.profoo.2011.09.085
- Sinelli, N., Benedetti, S., Bottega, G., Riva, M., Buratti, S., 2006. Evaluation of the optimal cooking time of rice by using FT-NIR spectroscopy and an electronic nose. *J. Cereal Sci.* 44, 137–143. doi:10.1016/j.jcs.2006.05.002
- Sun, Q., Han, Z., Wang, L., Xiong, L., 2014. Physicochemical differences between sorghum starch and sorghum flour modified by heat-moisture treatment. *Food Chem.* 145, 756–64. doi:10.1016/j.foodchem.2013.08.129
- Verdú, S., Ivorra, E., Sánchez, A.J., Barat, J.M., Grau, R., 2015a. Study of high strength wheat flours considering their physicochemical and rheological characterisation as well as fermentation capacity using SW-NIR imaging. *J. Cereal Sci.* 62, 31–37. doi:10.1016/j.jcs.2014.11.002
- Verdú, S., Ivorra, E., Sánchez, A.J., Barat, J.M., Grau, R., 2015b. Relationship between fermentation behavior, measured with a 3D vision Structured Light technique, and the internal structure of bread. *J. Food Eng.* 146, 227–233. doi:10.1016/j.jfoodeng.2014.08.014
- Verdú, S., Vásquez, F., Grau, R., Ivorra, E., Sánchez, A.J., Barat, J.M., 2016. Detection of adulterations with different grains in wheat products based on the hyperspectral image technique: The specific cases of flour and bread. *Food Control* 62, 373–380. doi:10.1016/j.foodcont.2015.11.002
- Wang, S., Karrech, A., Regenauer-Lieb, K., Chakrabati-Bell, S., 2013. Digital bread crumb: Creation and application. *J. Food Eng.* 116, 852–861. doi:10.1016/j.jfoodeng.2013.01.037
- Wu, D., He, Y., Feng, S., 2008. Short-wave near-infrared spectroscopy analysis of major compounds in milk powder and wavelength assignment. *Anal. Chim. Acta* 610, 232–242. doi:10.1016/j.aca.2008.01.056
- Wu, D., Sun, D.-W., 2013. Advanced applications of hyperspectral imaging technology for food quality and safety analysis and assessment: A review — Part I: Fundamentals. *Innov. Food Sci. Emerg. Technol.* 19, 1–14. doi:10.1016/j.ifset.2013.04.014
- Xing, J., Symons, S., Hatcher, D., Shahin, M., 2011. Comparison of short-wavelength infrared (SWIR) hyperspectral imaging system with an FT-NIR spectrophotometer for predicting alpha-amylase activities in individual Canadian Western Red Spring (CWRS) wheat kernels. *Biosyst. Eng.* 108, 303–310. doi:10.1016/j.biosystemseng.2011.01.002

Yao, H., Hruska, Z., Kincaid, R., Brown, R.L., Cleveland, T.E., 2008. Differentiation of toxigenic fungi using hyperspectral imagery. *Sens. Instrum. Food Qual. Saf.* 2, 215–224. doi:10.1007/s11694-008-9055-z

Zawa, M.O., Eguchi, M.S., n.d. Relationship between Pancake Springiness and Interaction of Wheat Flour Components Caused by Dry Heating.